NASA TECHNICAL NOTE

NASA TN D-

NASA TN D-4393

COLD-AIR PERFORMANCE EVALUATION OF SCALE MODEL OXIDIZER PUMP-DRIVE TURBINE FOR THE M-1 HYDROGEN-OXYGEN ROCKET ENGINE

IV - Performance of First Stage With Modified Inlet Feedpipe-Manifold Assembly

by Roy G. Stabe and John F. Kline

Lewis Research Center
Cleveland, Ohio

NATIONAL AERONAUTICS AND SPACE ADMINISTRATION • WASHINGTON, D. C. • FEBRUARY 1968

NASA TN D-4393

COLD-AIR PERFORMANCE EVALUATION OF SCALE MODEL OXIDIZER PUMP-DRIVE TURBINE FOR THE M-1 HYDROGEN-OXYGEN ROCKET ENGINE

IV - Performance of First Stage With Modified Inlet Feedpipe-Manifold Assembly

By Roy G. Stabe and John F. Kline

Lewis Research Center
Cleveland, Ohio

NATIONAL AERONAUTICS AND SPACE ADMINISTRATION

For sale by the Clearinghouse for Federal Scientific and Technical Information
Springfield, Virginia 22151 – CFSTI price $3.00

COLD-AIR PERFORMANCE EVALUATION OF SCALE MODEL OXIDIZER PUMP-DRIVE TURBINE FOR THE M-1 HYDROGEN-OXYGEN ROCKET ENGINE IV-PERFORMANCE OF FIRST STAGE WITH MODIFIED INLET FEEDPIPE-MANIFOLD ASSEMBLY

by Roy G. Stabe and John F. Kline

SUMMARY

The aerodynamic performance of a 0.45 scale-model of the first stage of the oxygen pump-drive turbine for the M-1 rocket engine was determined experimentally. These tests differed from previous tests of the first stage in that two additional feedpipes were installed in the turbine inlet manifold to improve the manifold performance. The first stage of the turbine was tested over a range of speeds and pressure ratios. The working fluid used in the investigation was dry air at inlet total conditions of 600° R (333° K) and approximately atmospheric pressure.

Modification of the inlet manifold reduced the average feedpipe Mach number from 0.274 to 0.172. As a result, the manifold total pressure loss was reduced from 5 percent of inlet total pressure to 2 percent of inlet total pressure. The circumferential variations in manifold and nozzle exit flow conditions were also much smaller with the modified than with the unmodified manifold.

The smaller total pressure loss in the modified inlet manifold increased the nozzle inlet total pressure, the nozzle pressure ratio, and the equivalent weight flow. At first-stage design equivalent speed and pressure ratio the equivalent weight flow was 6.65 pounds per second (3.02 kg/sec) compared to 6.31 pounds per second (2.86 kg/sec) with the unmodified manifold. With the modified manifold, the equivalent flow was still 6 percent less than the design value of 7.071 pounds per second (3.20 kg/sec). This deficit was attributed principally to a smaller than design nozzle throat area as well as flow conditions at the throat that differed somewhat from design.

At first stage design equivalent speed and blade-jet speed ratio, the static efficiency was 0.39 and the total efficiency was 0.64 compared to 0.37 and 0.57 for the first stage with the unmodified manifold. The total efficiency of the first stage based on nozzle inlet, rather than manifold inlet, total pressure was 0.69 with the modified manifold compared to 0.67 with the unmodified manifold.

An analysis of first-stage performance indicated that the rotor adiabatic efficiency increased from 0.81 with the unmodified inlet manifold to 0.84 with the modified inlet manifold. This improvement was attributed to the more uniform rotor inlet flow conditions afforded by the modified manifold. The nozzle adiabatic efficiency, however, was 0.94 for both cases.

INTRODUCTION

Experimental performance evaluations of the pump-drive turbines for the M-1 engine have been included as part of the turbine research and project support programs. The M-1 is a 1.5-million-pound-thrust (6.67×10^6 N) hydrogen-oxygen rocket engine. Fuel and oxidizer turbopumps are mounted on opposite sides of the engine combustion chamber. Each pump is driven by a two-stage velocity-compounded turbine.

Details of the fuel pump-drive turbine design may be found in reference 1. Cold-air performance evaluations of a 0.646 scale-model fuel turbine inlet feedpipe-manifold assembly, first stage, and complete two-stage turbine have been reported in reference 2. Details of the oxygen pump-drive turbine design may be found in reference 3.

Previous investigations of a 0.45 scale model of the oxygen pump-drive turbine include an experimental determination of the inlet manifold-nozzle performance (ref. 4), an experimental determination of the two-stage turbine performance (ref. 5), and an experimental determination of the performance of the first stage with the inlet feedpipe manifold assembly (ref. 6).

In reference 4 it was reported that the comparatively high velocities in the two inlet feedpipes and in the toroidal inlet manifold caused a larger than design loss in manifold total pressure and a substantial circumferential variation in nozzle exit flow conditions. The two-stage turbine and also the first stage were tested with this inlet manifold (refs. 5 and 6). In both cases the turbine efficiency was approximately as designed but the equivalent weight flow was 10.8 percent less than the design value. The reduction in equivalent weight flow was attributed to the larger than design inlet manifold total pressure loss, the circumferential variation in manifold flow conditions, and to less than design nozzle and first-stage rotor throat areas.

For the tests described in this report, the inlet manifold was modified by the installation of two additional feedpipes. Experience with the original inlet manifold indicated that this modification would result in lower total pressure loss and in improved distribution of the flow around the manifold circumference.

The performance of the modified inlet feedpipe manifold-nozzle assembly was investigated by means of circumferential surveys of nozzle exit total pressure at several pressure ratios. The results of these tests are compared with the results of similar tests performed on the unmodified assembly which were reported in reference 4.

The first-stage turbine configuration, with the modified inlet manifold assembly, was then tested at constant speeds of 60, 80, 90, 100, and 110 percent of design equivalent speed and over a range of pressure ratios from 1.2 to 2.0. Zero-speed torque data were obtained for a similar range of pressure ratios. Radial surveys of rotor exit flow conditions were performed at design equivalent speed and pressure ratio. First-stage performance in terms of weight flow, specific work, static efficiency, and torque are presented

for the range of speeds and pressure ratios covered in the investigation.

First-stage velocity diagrams, losses, and blade performance parameters at design speed and pressure ratio are compared with the corresponding results of the first-stage test with the unmodified manifold which were reported in reference 6.

SYMBOLS

A	area, sq in. (sq m)
g_c	dimensional conversion constant, 32.17 ft-lb/(lb)(sec^2)
h	specific enthalpy, Btu/lb (J/g)
$\Delta h'$	turbine specific work, Btu/lb (J/g)
J	mechanical equivalent of heat, 778 ft-lb/Btu
M	Mach number
p	absolute pressure, lb/sq in. (N/sq cm)
r	radius, in. (m)
U_m	mean diameter blade speed, ft/sec (m/sec)
V	absolute velocity, ft/sec (m/sec)
W	velocity relative to rotor blade, ft/sec (m/sec)
w	weight flow, lb/sec (kg/sec)
α	absolute flow angle measured from axial direction, deg
β	relative flow angle measured from axial direction, deg
γ	ratio of specific heats
δ	ratio of inlet total pressure to standard sea-level pressure, $p'_1/14.696$ lb/sq in. ($p'_1/10.132$ N/sq cm)
ϵ	gamma (γ) correction function, $\left(\frac{0.74}{\gamma}\right)\left(\frac{\gamma+1}{2}\right)^{\gamma/(\gamma-1)}$
η	static efficiency, $\Delta h' \Big/ \left(h'_1 - h_4\right)_s$
η_N	nozzle adiabatic efficiency, $\left(h'_2 - h_3\right) \Big/ \left(h'_2 - h_3\right)_s$
η_R	rotor adiabatic efficiency, $\left(h''_3 - h_4\right) \Big/ \left(h''_3 - h_4\right)_s$
$\sqrt{\theta_{cr,1}}$	ratio of turbine inlet critical velocity to critical velocity of standard sea level air, $V_{cr,1}/1019$, ft/sec ($V_{cr,1}/310.6$, m/sec)

ν	blade-jet speed ratio, $U_m \Big/ \sqrt{2g_c J \left(h'_1 - h_4\right)_s}$
τ	torque, lb-ft (N-m)

Subscripts:

ann	annulus
cr	conditions corresponding to those at a Mach number of 1
s	isentropic or ideal process
t	blade tip section
th	throat
1, 2, 3, 4, 4a	measuring stations (see fig. 1)

Superscripts:

$(\bar{})$	arithmetic average value
'	absolute total state condition
''	total state condition relative to rotor blade

APPARATUS AND PROCEDURE

The 0.45 scale-model turbine and the test facility with which the performance of the M-1 oxidizer pump-drive turbine first stage was evaluated (ref. 6) were used for this investigation.

The turbine inlet manifold was modified by the installation of two additional feedpipes diametrically opposite the existing two. A sketch of the cross section through the modified manifold is shown in figure 1. The axial and circumferential location of the instrumentation is also shown in figure 1.

For tests of the feedpipe-manifold-nozzle configuration, a Kiel-type total pressure probe set at the design flow angle was located 1/8 inch (0.318 cm) axially downstream from the nozzle exit. The probe and the circumferential survey equipment are described in reference 4.

For tests of the first-stage configuration, four combination (flow-angle and total-pressure) radial-survey probes were located around the circumference one axial blade chord downstream from the rotor exit.

Airflow rate was measured with a calibrated ASME thin-plate orifice run. Orifice inlet pressure was measured with a calibrated precision Bourdon tube gage. All other

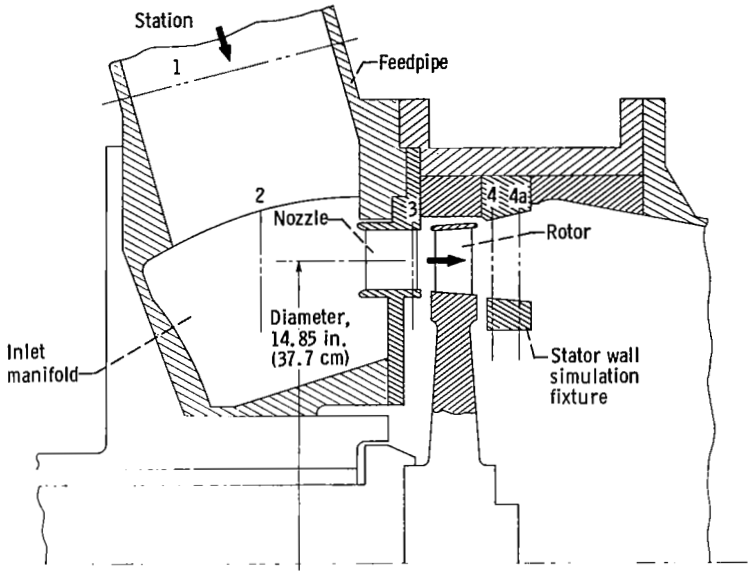

Cross section of first-stage turbine configuration.

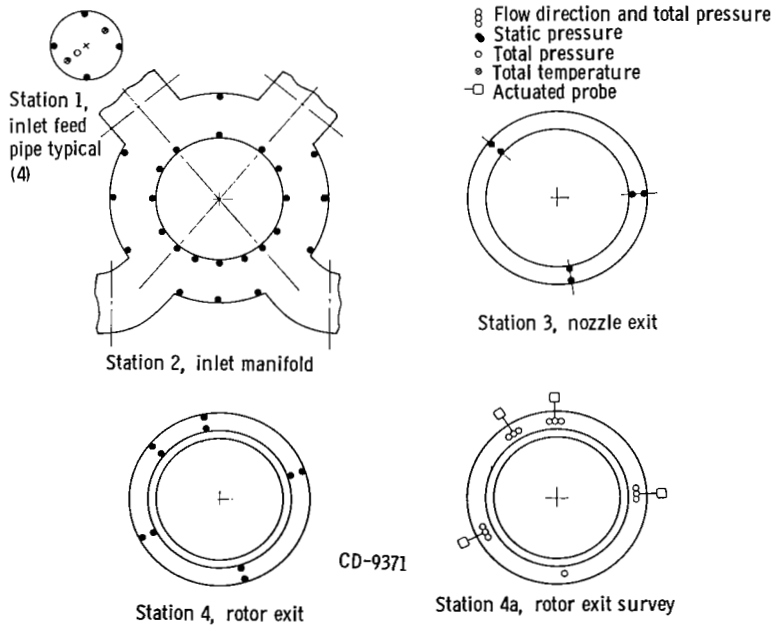

Views looking upstream.

Figure 1. - Location of instrumentation and station nomenclature.

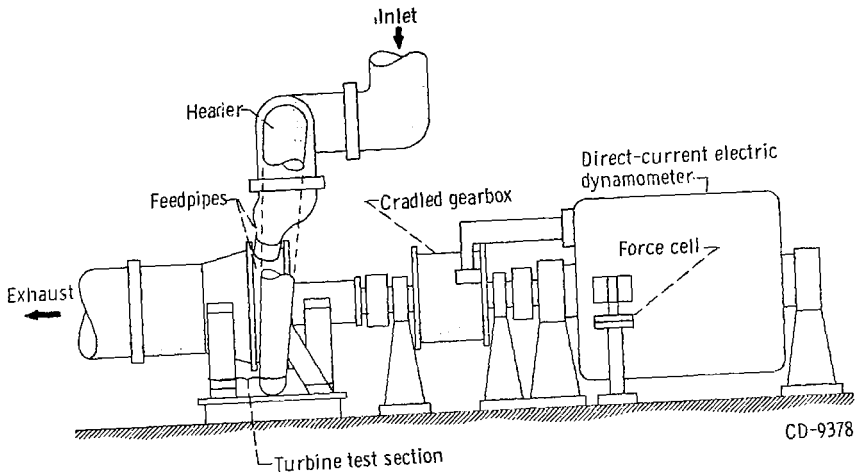

(a) Schematic diagram.

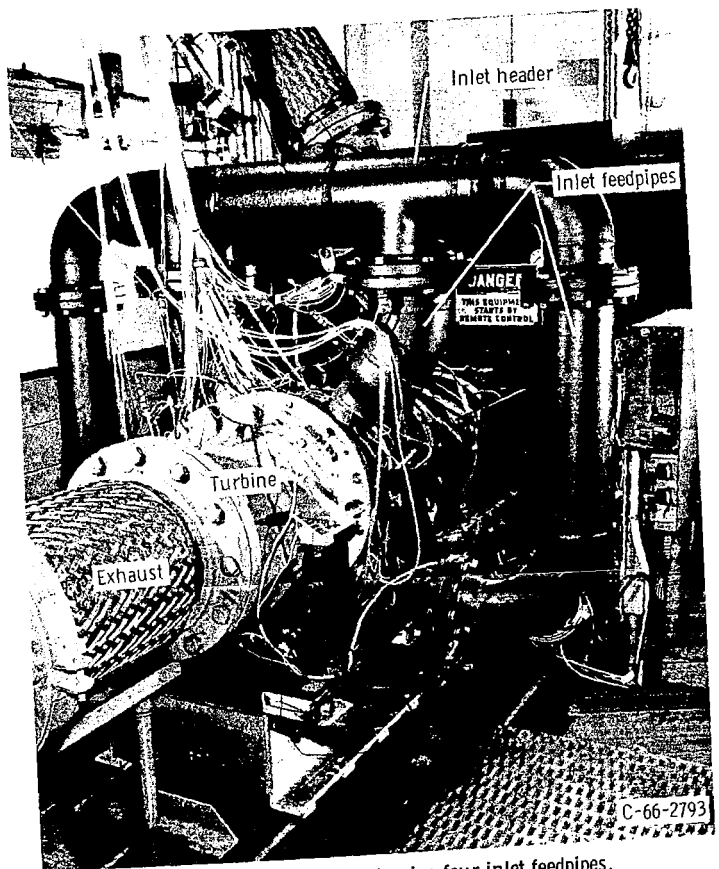

(b) Turbine installation showing four inlet feedpipes.

Figure 2. - Turbine test facility.

pressures were recorded simultaneously by photographing a bank of mercury manometers. Temperatures were read on an industrial self-balancing potentiometer. Turbine rotative speed was measured with an electronic counter in conjunction with a magnetic pickup and a 60-tooth gear mounted on the turbine shaft. The total reaction torque of the gear-box and dynamometer was measured with a strain-gage force cell in conjunction with an integrating digital millivoltmeter.

A diagram and overall view of the test facility are shown in figure 2. Turbine output torque is transmitted through a cradled gear box to a cradled direct-current dynamometer.

All tests were conducted with dry air at a total pressure of 30 inches of mercury (10.16 N/sq cm) absolute and a temperature of 600° R (333° K) at station 1 in the manifold feedpipes.

The inlet manifold-nozzle assembly was tested separately at pressure ratios (inlet total to nozzle exit static) from 1.2 to 2.0. Nozzle exit total pressure was surveyed circumferentially at three radial positions at each pressure ratio. This procedure is described in reference 4.

The first stage of the turbine was operated at 0, 60, 80, 90, 100, and 110 percent of design equivalent speed at pressure ratios from 1.2 to 2.0. Rotor exit flow conditions were surveyed radially at four circumferential stations and at design equivalent speed and pressure ratio. The torque measuring system was calibrated in place before and after each day's operation by dead-weight loading the dynamometer stator.

Turbine specific work $\Delta h'$ was calculated from weight flow, speed, and turbine torque data. Turbine torque was determined by adding bearing-seal torque (approximately 2 percent of design equivalent first-stage torque) to the torque indicated by the force cell. Bearing-seal torque was determined directly by removing the rotor and motoring the test unit at each speed.

Inlet (feedpipe) average total pressure p'_1 was calculated from the average static pressure and temperature and the total flow area and weight flow in the four feedpipes.

The pressure ratio used to determine turbine performance is based on the average inlet total pressure p'_1 and the average of the hub and tip static pressures at the rotor exit $\bar{p}_4$ (station 4).

RESULTS AND DISCUSSION

The results of the cold-air performance evaluation of the scale-model oxidizer turbine first stage with the modified inlet manifold are presented in the following sections: Inlet Manifold-Nozzle Assembly, First-Stage Performance, and Analysis of First-Stage

Performance. Where appropriate, the results of this investigation are compared with the results of the investigation of the first stage with the original or unmodified manifold reported in reference 6.

Inlet Manifold-Nozzle Assembly

The performance of the modified inlet manifold-nozzle assembly was investigated by means of circumferential surveys of nozzle exit total pressure at several pressure ratios. The same procedure was used in the investigation of the unmodified manifold. In this report, as in reference 4, it is assumed that the maximum total pressure recorded at the exit of each nozzle channel is representative of the effective total pressure in the manifold at the entrance of the respective nozzle channels.

Nozzle exit total pressure surveys. - A strip chart record of a typical nozzle exit survey, made at the nozzle mean diameter, is reproduced in figure 3(a). For compari-

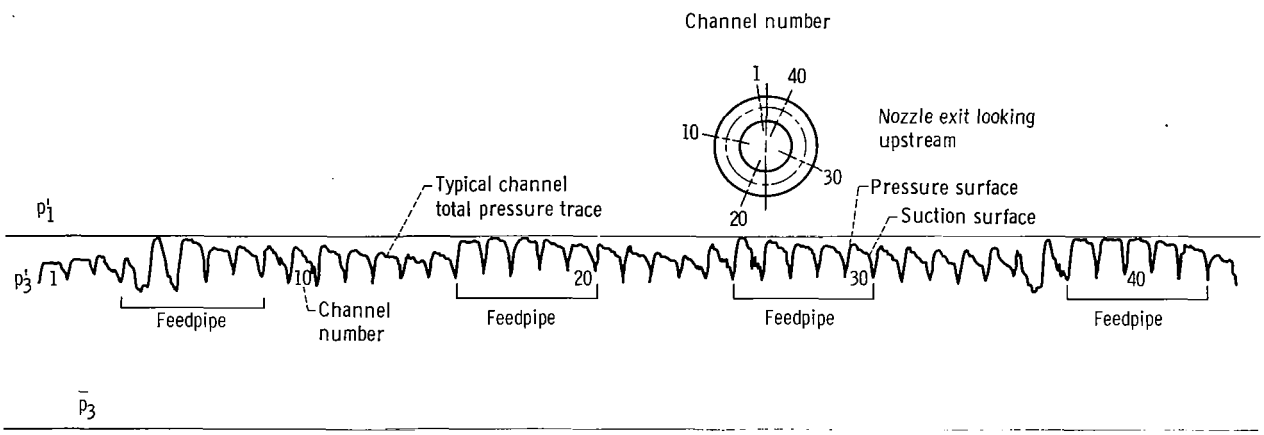

(a) With modified (4-feedpipe) manifold. Equivalent inlet total to nozzle exit static pressure ratio, 1.53.

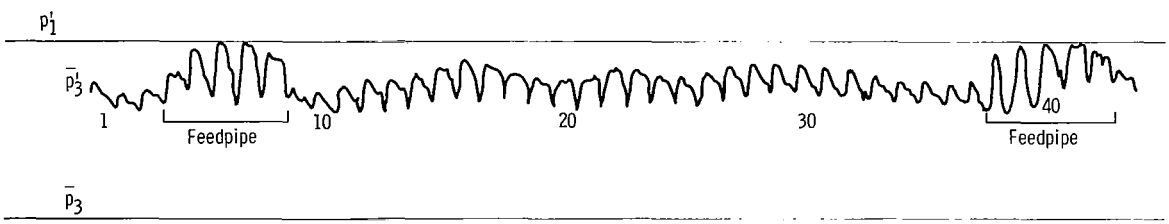

(b) With original (2-feedpipe) manifold. Equivalent inlet total to nozzle exit static pressure ratio, 1.48.

Figure 3. - Comparison of circumferential surveys of nozzle exit total pressure at mean diameter.

son, a record of a similar survey made with the unmodified manifold is reproduced in figure 3(b). The level of inlet total pressure and nozzle exit static pressure, relative to the nozzle exit total pressure trace, is indicated. The vertical or pressure scale is the same for both survey records. The location of the manifold feedpipes and several nozzle channels is also shown.

The total pressure traces shown in figure 3 indicate that the performance of the modified inlet manifold-nozzle assembly is generally superior to the performance of the unmodified assembly. The most significant improvements are the greatly reduced circumferential variation of nozzle inlet total pressure, as indicated by the envelope of the maximum nozzle channel total pressures, and the higher average nozzle inlet total pressure.

Manifold total pressure loss. - The average manifold total pressure $\bar{p}_2'$ is the average of the maximum nozzle channel exit total pressures. The manifold total pres-

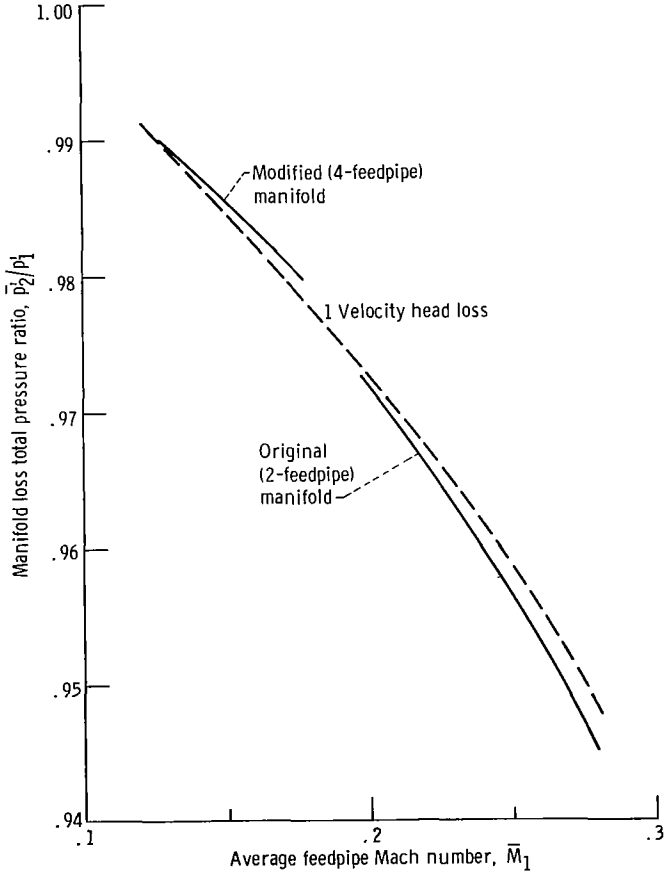

Figure 4. - Inlet manifold total pressure loss as a function of feedpipe Mach number.

sure ratio $\overline{p}_2'/p_1'$ for both modified and unmodified manifolds is shown as a function of average feedpipe Mach number in figure 4. A total pressure ratio corresponding to a loss of one feedpipe velocity head is also shown in this figure as a dashed line. The total pressure loss for both modified and unmodified manifolds is very nearly equal to a loss of one feedpipe velocity head. At first-stage design pressure ratio, the average feedpipe Mach number is 0.172 for the modified manifold and 0.274 for the unmodified manifold. The corresponding manifold total pressure ratios $\overline{p}_2'/p_1'$ are very nearly 0.98 and 0.95 for the modified and unmodified manifolds, respectively.

First-Stage Performance

The first-stage turbine configuration, with the modified inlet manifold, was tested at constant speeds of 0, 60, 80, 90, 100, and 110 percent of design equivalent speed and over a range of pressure ratios from 1.2 to 2.0.

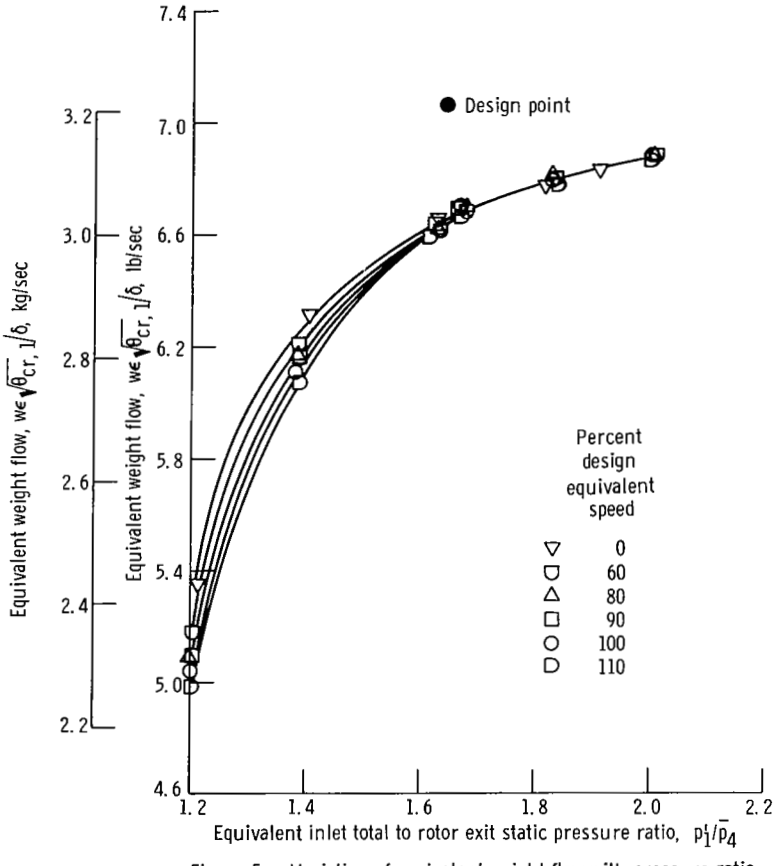

Figure 5. - Variation of equivalent weight flow with pressure ratio and speed.

Weight flow. - Equivalent weight flow is plotted against equivalent pressure ratio and speed in figure 5. At first-stage design equivalent pressure ratio (1.646) and speed, the equivalent weight flow was 6.65 pounds per second (3.02 kg/sec) which is 6 percent less than the design value of 7.071 pounds per second (3.20 kg/sec). The equivalent weight flow for the first stage with the original manifold at the same speed and pressure ratio was 6.31 pounds per second (2.86 kg/sec), 10.8 percent less than design. This 5.4 percent increase in weight flow is largely due to a higher average nozzle inlet total pressure and a higher nozzle total- to static-pressure ratio which resulted from the lower total pressure loss in the modified inlet manifold than in the original manifold.

Equivalent specific work. - Equivalent specific work as a function of equivalent pressure ratio and speed is shown in figure 6. At first-stage design equivalent pressure

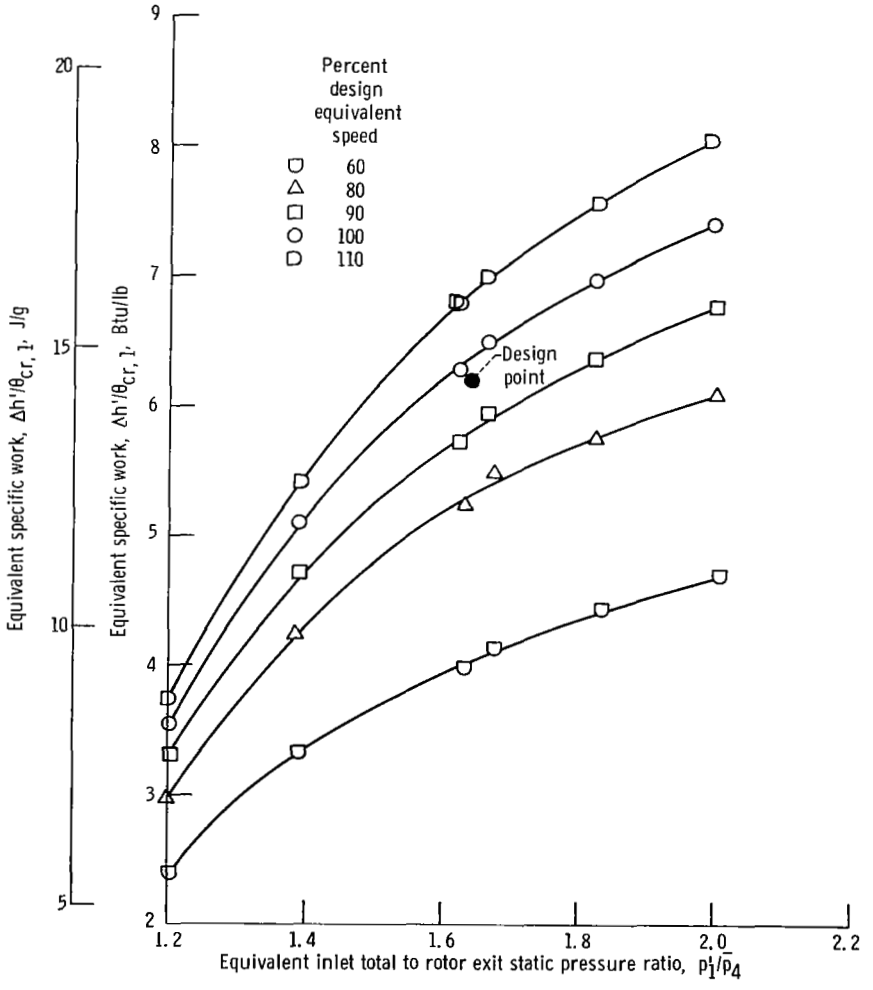

Figure 6. - Variation of first-stage equivalent specific work with pressure ratio and speed.

ratio and speed, the equivalent specific work of the first stage is 6.4 Btu per pound (14.9 J/g) compared to 6.15 Btu per pound (14.3 J/g) for the first stage with the original inlet manifold. The continued upward trend of the equivalent specific work curves at the higher pressure ratios indicates that the first stage was not operating near limiting loading.

Static efficiency. - First-stage static efficiency as a function of blade-jet speed ratio and percent design equivalent speed is shown in figure 7. At first-stage design equivalent speed and blade-jet speed ratio (0.135), the static efficiency is 0.39 compared to 0.37 for the original first-stage configuration and the design value of 0.375.

Equivalent torque. - Equivalent torque as a function of percent design equivalent speed and pressure ratio is shown in figure 8. These curves were constructed from plots of equivalent torque against equivalent pressure ratio for constant speeds of 0, 60, 80, 90, 100, and 110 percent of design equivalent speed.

The equivalent torque of the first stage at design equivalent speed and pressure ratio is 167 pound-feet (226 N-m) compared to 152 pound-feet (206 N-m) reported in reference 6 for the first stage with the unmodified manifold and 172 pound-feet (233 N-m) design. The increase in equivalent torque over that of the first stage with the unmodified manifold is due to the higher efficiency and weight flow obtained with the modified

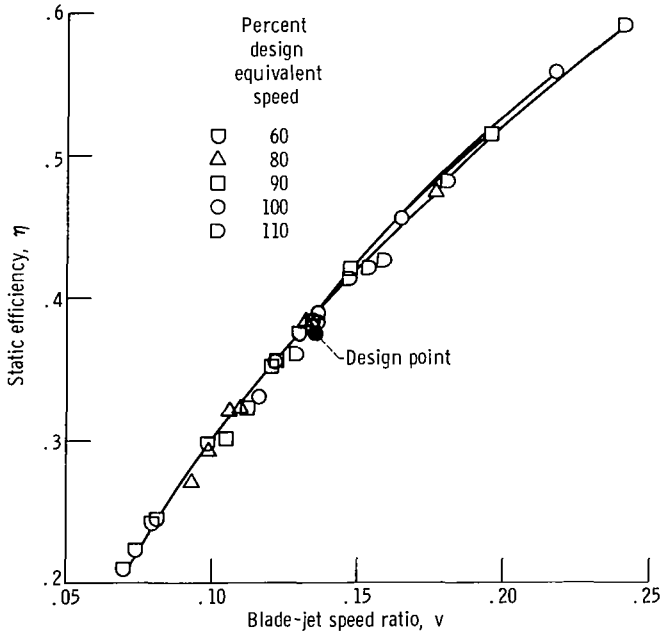

Figure 7. - Variation of first-stage static efficiency with blade-jet speed ratio and speed.

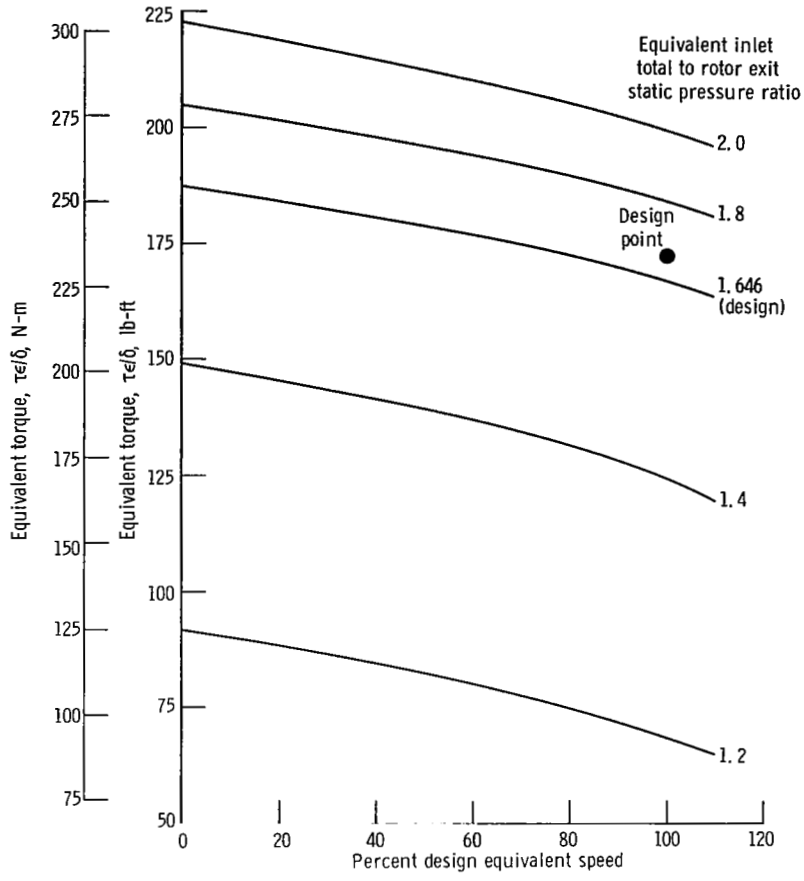

Figure 8. - Variation of first-stage equivalent torque with speed and pressure ratio.

inlet manifold. Design equivalent torque was not achieved because the equivalent weight flow is still 6 percent less than design. At design equivalent pressure ratio, the ratio of zero speed to design speed equivalent torque is 1. 12. This ratio is small because of the very low first-stage blade-jet speed ratio.

First-stage rotor exit surveys. - Radial surveys of first-stage rotor exit flow conditions were made at design equivalent speed and nominally design equivalent pressure ratio. Absolute flow angle and total pressure were measured at four circumferential positions and at several radial locations along the blade span.

The radial variation in first-stage rotor exit absolute flow angle and rotor exit total to inlet total pressure ratio p'_4/p'_1 are shown in figure 9. The data shown in figure 9 represent the circumferential average of the four measurements taken at each radial location. The radial variation of both first-stage rotor exit angle and total pressure ratio are very similar to those reported for the first stage with the unmodified manifold in reference 6.

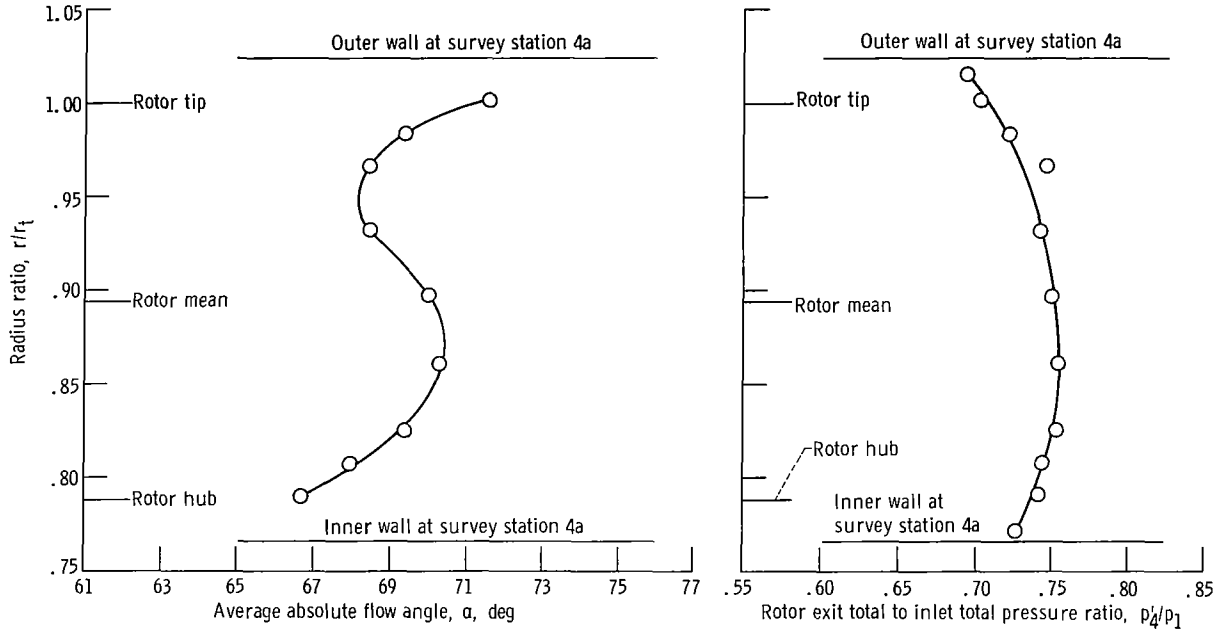

(a) Radial variation of first-stage rotor exit flow angle.

(b) Radial variation of first-stage rotor exit total pressure.

Figure 9. - First-stage rotor exit surveys at design equivalent speed and approximately design equivalent pressure ratio.

The spanwise integrated average values of flow angle and rotor exit total to inlet total pressure ratio are 69.3° and 0.742, respectively, compared to 69.8° and 0.724, respectively, reported in reference 6 for the first stage with the original manifold.

Analysis of First-Stage Performance

First-stage velocity diagrams, losses, and blade performance parameters at design equivalent speed and approximately design equivalent pressure ratio were computed and are compared with the corresponding results of the first-stage test with the unmodified manifold as reported in reference 6.

Velocity diagrams. - A velocity diagram representative of the first-stage performance was calculated from test data. The data used were for design equivalent speed and an equivalent pressure ratio $p'_1/\bar{p}_4$ of 1.668. The rotor exit velocity was calculated from the average values of rotor exit static and total pressures. The average values of the first-stage exit flow angle and mean diameter blade speed were used to complete the exit velocity triangle. The rotor inlet tangential velocity was then specified by the measured specific work. The rotor inlet axial velocity was calculated from continuity.

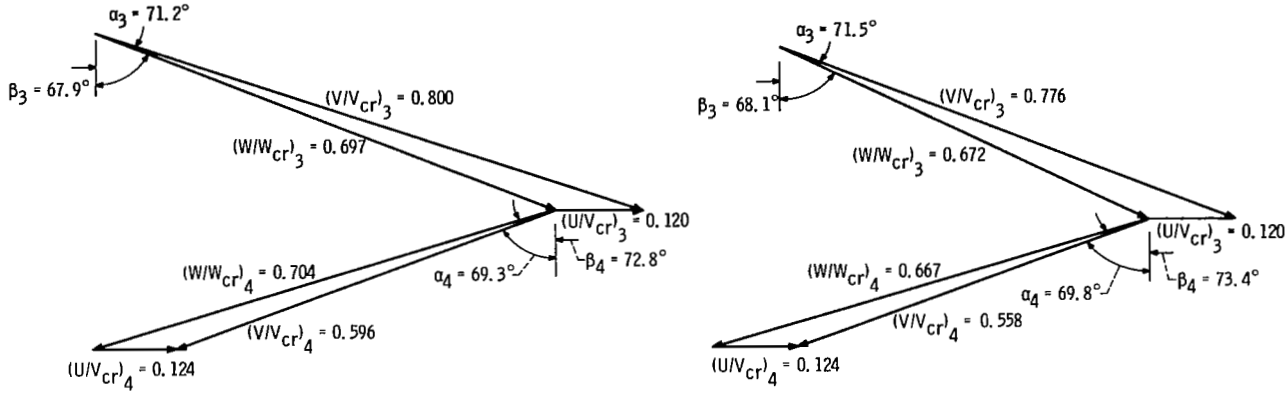

(a) For modified (4-feedpipe) manifold.

(b) For unmodified (2-feedpipe) manifold.

Figure 10. - First-stage mean diameter velocity diagrams calculated from test data at design equivalent speed and approximately design equivalent pressure ratio.

Nozzle exit area, weight flow, and average nozzle exit static pressure data were used for this calculation. This diagram is presented in figure 10(a). For comparison, the velocity diagram obtained for the first stage with the unmodified manifold (ref. 6) is shown in figure 10(b).

The most significant difference between these two velocity diagrams are the nozzle and rotor exit velocities. The velocities for the first stage with the modified manifold are higher than the corresponding velocities for the first stage with the unmodified manifold. These higher velocities resulted in the increased specific work and static efficiency reported in previous sections.

The rotor reaction, implied by the difference between the rotor inlet and exit relative velocities, is small but positive for the modified manifold case and equally small but negative for the unmodified manifold case. The rotor inlet and exit angles β_3 and β_4 are also nearly the same for both cases.

Axial pressure distribution. - The axial distribution of absolute and relative total to inlet total pressure ratios corresponding to the velocity diagrams of figure 10 are shown in figure 11(a). The axial distribution of average static to inlet total pressure ratios for the two first-stage configurations is shown in figure 11(b).

The average absolute and relative total pressures for the modified manifold first-stage configuration are all higher than the corresponding pressures of the unmodified manifold case. The higher total pressure level obtained with the modified manifold results from the initial advantage of the smaller manifold total pressure loss. The rotor relative total pressure losses are nearly equal for both configurations. And the nozzle total pressure loss is slightly higher for the modified case than for the unmodified. The nozzle total pressure ratio $\overline{p}'_3/\overline{p}'_2$ is 0.972 with the modified manifold and 0.976 with the unmodified manifold.

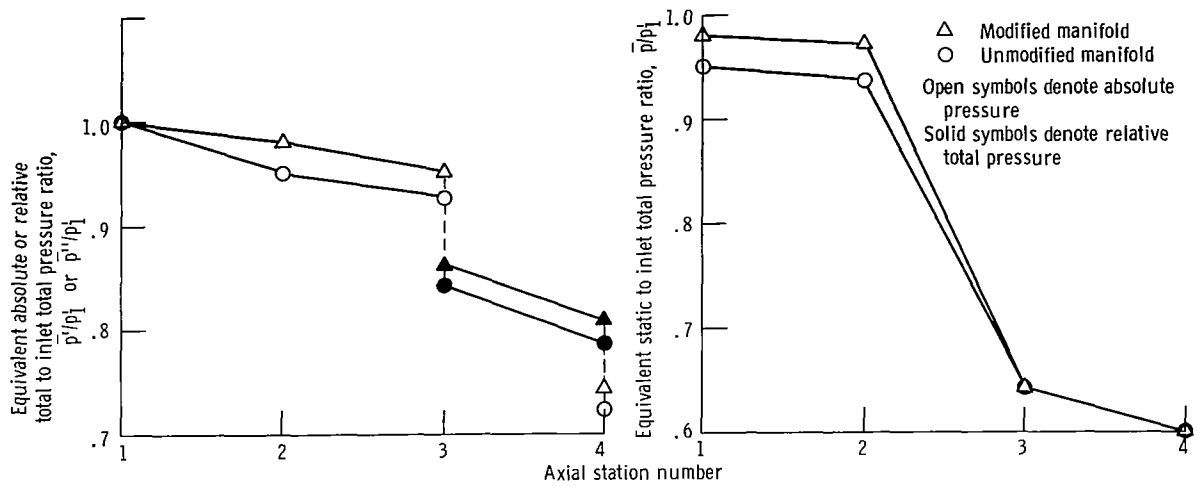

(a) Total pressure.

(b) Static pressures.

Figure 11. - Axial distribution of average static and total pressures at design equivalent speed and approximately design equivalent pressure ratio.

The static pressure level, figure 11(b), at the inlet and exit of the rotor is the same for both configurations. The inlet total to exit static pressure ratios for both nozzle and rotor are then higher for the first stage with the modified manifold than with the unmodified manifold. The higher inlet total to exit static pressure ratios are compatable with the higher velocities and also the larger equivalent weight flow obtained with the modified manifold.

Utilization of available energy. - The velocity diagram and pressure data of figures 10 and 11 were used to calculate the losses in available energy resulting from the nonisentropic processes that occurred in the manifold, nozzle, and first-stage rotor. The ratio of work or loss to the ideal available energy for both first-stage configurations are compared in figure 12.

The sum of the work and the leaving energy is 0.797 for the first stage with the modified manifold compared to 0.735 for the first stage with the unmodified manifold. That is, the first stage with the modified manifold either converted to work or made available to a succeeding stage 79.7 percent of the energy available to it. The increased utilization of available energy indicates that there was also an increase in first-stage total efficiency. The total efficiency of the first stage with the modified manifold was 0.64 compared to 0.57 for the first stage with the unmodified manifold.

The modification of the inlet manifold reduced the manifold loss from 9.5 to 3.7 percent of first-stage available energy. This reduction in manifold loss is the principal reason for the large increase in first-stage total efficiency. The total efficiencies ex-

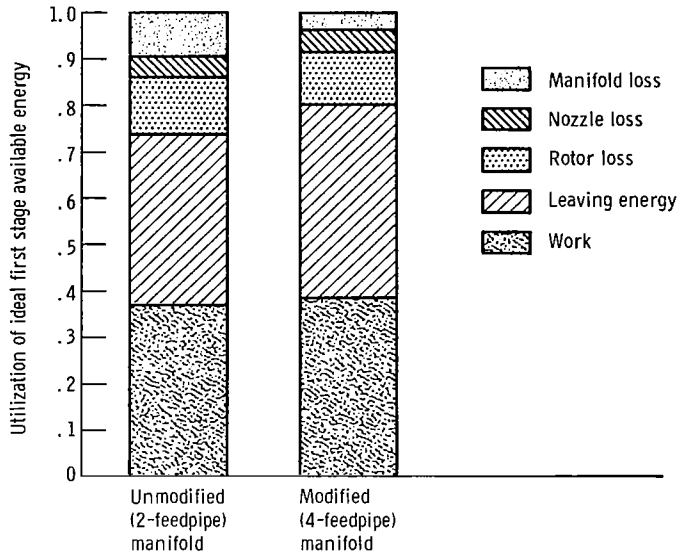

Figure 12. - Utilization of ideal available energy of first stage with modified and unmodified inlet manifolds.

clusive of the manifold, that is, the total efficiency based on the nozzle inlet to rotor exit total pressure ratio $\overline{p}'_2/\overline{p}'_4$ are 0.69 and 0.67 for the first stage with the modified and unmodified manifolds, respectively.

The nozzle loss with the modified manifold was 5.2 percent of the available energy compared to 4.5 percent with the unmodified manifold. However, the nozzle adiabatic efficiency η_N was found to be 0.94 for both the modified and unmodified manifold cases. For a given nozzle adiabatic efficiency, the loss is dependent only on pressure ratio. And, as mentioned in the section, Axial pressure distribution, the nozzle pressure ratio was larger with the modified manifold. Therefore, the loss was larger also.

The rotor loss, with the modified manifold, was 11.4 percent of available energy compared to 12.7 percent with the unmodified manifold. The corresponding rotor adiabatic efficiencies η_R are 0.84 and 0.81 for the modified and unmodified manifold cases, respectively. This increase in rotor adiabatic efficiency is the reason for the increase in first-stage total efficiency (exclusive of the inlet manifold) mentioned previously.

This improvement in rotor adiabatic efficiency is attributed principally to the more uniform inlet conditions obtained with the modified manifold. In addition, the level of rotor adiabatic efficiency is quite high, particularly in view of the thick blunt leading edge blades used for the rotor.

Nozzle performance. - The more uniform nozzle inlet flow conditions obtained with the modified inlet manifold did not result in an improvement in nozzle adiabatic efficiency. At design equivalent speed and overall first-stage pressure ratio, the nozzle efficiency is 0.94 with either the modified or unmodified inlet manifold. Design nozzle efficiency was 0.91.

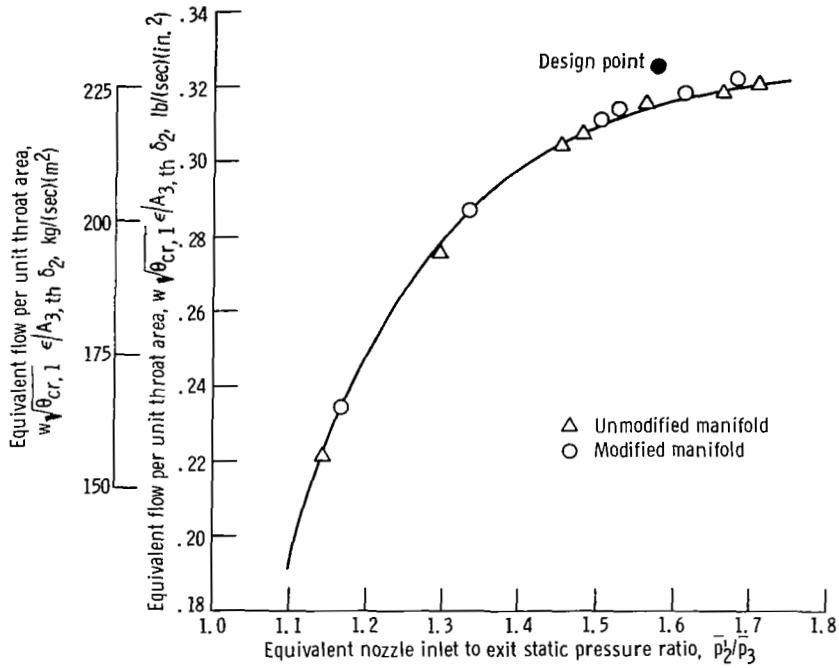

Figure 13. - Comparison of actual and theoretical variation of nozzle equivalent flow per unit throat area with nozzle pressure ratio.

Another aspect of nozzle performance is the weight flow per unit area. The ratio of equivalent weight flow to the nozzle throat area is plotted against nozzle pressure ratio in figure 13. Data for the first stage with the modified and unmodified inlet manifolds are shown. In figure 13, the equivalent weight flow is referenced to the nozzle inlet total pressure $\bar{p}'_2$ rather than manifold inlet total pressure p'_1. The data shown in the figure indicate that the weight flow characteristics of the nozzle were essentially the same with either the modified or unmodified inlet manifold.

The dependent variable of figure 13 is a function of the nozzle pressure ratio $\bar{p}'_2/\bar{p}_3$, the nozzle adiabatic efficiency η_N, the nozzle annulus to throat area ratio $A_{3,ann}/A_{3,th}$ and the nozzle exit flow angle $\bar{\alpha}_3$. Therefore,

$$\frac{w\sqrt{\theta_{cr,1}}\,\epsilon}{A_{3,th}\,\delta_2} = C\,\frac{\gamma\epsilon}{\sqrt{\gamma^2-1}}\,\frac{A_{3,ann}}{A_{3,th}}\cos\bar{\alpha}_3\,\frac{\left[\left(\frac{\bar{p}'_2}{\bar{p}_3}\right)^{-2/\gamma} - \left(\frac{\bar{p}'_2}{\bar{p}_3}\right)^{-(\gamma+1)/\gamma}\right]^{1/2}}{\sqrt{\eta_N}\left[\frac{1-\eta_N}{\eta_N}\left(\frac{\bar{p}'_2}{\bar{p}'_3}\right)^{(\gamma-1)/\gamma} + 1\right]} \qquad (1)$$

where C = 0.928 pounds per second per square inch and is a function of standard sea-level pressure and critical velocity. If the International System of Units is used, C = 652.4 kilograms per second per square meter.

The nozzle annulus to throat area ratio is 3.065. This is larger than the design value which was 2.971 because the scale-model throat area was smaller than design. The average nozzle exit flow angle from the velocity diagrams (fig. 10) is 71.35°. The exit flow angle is also larger than the design value which was 70.0°. Equation (1) was evaluated for the constant values of $\eta_N = 0.94$, $A_{3,ann}/A_{3,th} = 3.065$, and $\overline{\alpha}_3 = 71.35^{\circ}$ and over a range of nozzle pressure ratios.

The resulting curve is also shown in figure 13 and is seen to fit the data for both manifolds very well. Thus it can be concluded that not only are the nozzle efficiency and exit flow angles comparable for the two manifolds, but also that these efficiencies and flow angles were very nearly constant over the range of pressure ratios investigated.

At design nozzle pressure ratio 1.58 the equivalent flow per unit throat area is 0.315 pound per second per square inch (222 kg/(sec)(sq m)) which is about 3.1 percent less than the design value of 0.325 pound per second per square inch (229 kg/(sec)(sq m).

This additional deficit in weight flow is attributed to flow conditions at the throat that differ somewhat from those of design (Mach number, static pressure, flow coefficient, etc.).

This flow deficit is also evidenced by the larger than design nozzle exit flow angle. At 70° the cosine function decreases rapidly so that a small increase in angle causes a fairly large decrease in the nozzle exit to throat area ratio (the term $(A_{3,ann}/A_{3,th}) \cos \overline{\alpha}_3$ in eq. (1)).

SUMMARY OF RESULTS

The aerodynamic performance of a 0.45 scale model of the first stage of the oxygen pump-drive turbine for the M-1 rocket engine was determined experimentally. These tests differed from previous tests of the first stage in that two additional feedpipes were installed in the turbine inlet manifold to improve the manifold performance. The first stage of the turbine was tested over a range of speeds and pressure ratios. The working fluid used in the investigation was dry air at inlet total conditions of 600° R (333° K) and approximately atmospheric pressure. The results of this investigation are summarized as follows:

1. Modification of the inlet manifold reduced the average feedpipe Mach number from 0.274 to 0.172. As a result, the manifold total pressure loss was reduced from 5 percent of inlet total pressure to 2 percent of inlet total pressure. The circumferential varia-

tions in manifold and nozzle exit flow conditions were also much smaller with the modified than with the unmodified manifold.

2. The smaller total pressure loss in the modified inlet manifold increased the nozzle inlet total pressure, the total-to static-pressure ratio, and the equivalent weight flow. At first-stage design equivalent speed and pressure ratio the equivalent weight flow was 6.65 pounds per second (3.02 kg/sec) compared to 6.31 pounds per second (2.86 kg/sec) with the unmodified manifold. With the modified manifold, the equivalent flow was still 6 percent less than the design value of 7.071 pounds per second (3.20 kg/sec). This deficit was attributed principally to a smaller than design nozzle throat area as well as flow conditions at the throat which differed somewhat from design.

3. At first-stage design equivalent speed and blade-jet speed ratio the static efficiency was 0.39 and the total efficiency was 0.64 compared to 0.37 and 0.57 for the first stage with the unmodified manifold. The total efficiency of the first stage based on nozzle inlet, rather than manifold inlet, total pressure was 0.69 with the modified manifold compared to 0.67 with the unmodified manifold.

4. An analysis of first-stage performance indicated that the rotor adiabatic efficiency increased from 0.81 with the unmodified inlet manifold to 0.84 with the modified inlet manifold. This improvement was attributed to the more uniform rotor inlet flow conditions afforded by the modified manifold. The nozzle adiabatic efficiency, however, was 0.94 for both cases.

Lewis Research Center,
National Aeronautics and Space Administration,
Cleveland, Ohio, October 18, 1967,
128-31-02-25-22.

REFERENCES

1. Reynolds, T. W.: Aerodynamic Design-Model II Turbine M-1 Fuel Turbopump Assembly. Rep. No. AGC-8800-52 (NASA CR 54820), Aerojet General Corp., Apr. 15, 1966.

2. Stabe, Roy G.; Kline, John F.; and Gibbs, Edward H.: Cold-Air Performance Evaluation of a Scale-Model Fuel Pump Turbine for the M-1 Hydrogen-Oxygen Rocket Engine. NASA TN D-3819, 1967.

3. Beer, R.: Aerodynamic Design and Estimated Performance of a Two-Stage Curtis Turbine for the Liquid Oxygen Turbopump of the M-1 Engine. Rep. No. AGC-8800-12 (NASA CR-54764), Aerojet General Corp., Nov. 19, 1965.

4. Stabe, Roy G.; Evans, David G.; and Roelke, Richard J.: Cold-Air Performance Evaluation of Scale Model Oxidizer Pump-Drive Turbine for the M-1 Hydrogen-Oxygen Rocket Engine. I - Inlet Feedpipe-Manifold Assembly. NASA TN D-3294, 1966.

5. Roelke, Richard J.; Stabe, Roy G.; and Evans, David G.: Cold-Air Performance Evaluation of Scale Model Oxidizer Pump-Drive Turbine for the M-1 Hydrogen-Oxygen Rocket Engine. II - Overall Two-Stage Performance. NASA TN D-3368, 1966.

6. Stabe, Roy G.; and Kline, John F.: Cold-Air Performance Evaluation of Scale Model Oxidizer Pump-Drive Turbine for the M-1 Hydrogen-Oxygen Rocket Engine. III - Performance of First Stage with Inlet-Feedpipe-Manifold Assembly. NASA Technical Note; estimated publication date, January 1968.

NASA-Langley, 1968 —— 28 E-4039

"The aeronautical and space activities of the United States shall be conducted so as to contribute . . . to the expansion of human knowledge of phenomena in the atmosphere and space. The Administration shall provide for the widest practicable and appropriate dissemination of information concerning its activities and the results thereof."

—NATIONAL AERONAUTICS AND SPACE ACT OF 1958

NASA SCIENTIFIC AND TECHNICAL PUBLICATIONS

TECHNICAL REPORTS: Scientific and technical information considered important, complete, and a lasting contribution to existing knowledge.

TECHNICAL NOTES: Information less broad in scope but nevertheless of importance as a contribution to existing knowledge.

TECHNICAL MEMORANDUMS: Information receiving limited distribution because of preliminary data, security classification, or other reasons.

CONTRACTOR REPORTS: Scientific and technical information generated under a NASA contract or grant and considered an important contribution to existing knowledge.

TECHNICAL TRANSLATIONS: Information published in a foreign language considered to merit NASA distribution in English.

SPECIAL PUBLICATIONS: Information derived from or of value to NASA activities. Publications include conference proceedings, monographs, data compilations, handbooks, sourcebooks, and special bibliographies.

TECHNOLOGY UTILIZATION PUBLICATIONS: Information on technology used by NASA that may be of particular interest in commercial and other non-aerospace applications. Publications include Tech Briefs, Technology Utilization Reports and Notes, and Technology Surveys.

Details on the availability of these publications may be obtained from:

SCIENTIFIC AND TECHNICAL INFORMATION DIVISION

NATIONAL AERONAUTICS AND SPACE ADMINISTRATION

Washington, D.C. 20546